

Vascular Characterization of Bone Metastasis in a Breast Cancer Animal Model by DCE-MRI

M. Dadiani¹, R. Margalit¹, O. Brener¹, H. Degani¹

¹Weizmann Institute of Science, Rehovot, Israel

Introduction

The main cause of mortality from breast cancer is related the dispersion of cancer to distant sites of the body, metastasis. In order to successfully metastasize, cancer cells must detach themselves from their original location, invade a blood or lymphatic vessel, travel in the circulation to a distant site and then establish a new cellular colony (1). Two major factors determine the dissemination of cancers to distant organs: the environment of the metastatic target site, and the properties of the cancer cells (2). In breast cancer, the most common sites of metastatic disease are the bones, lungs, liver and lymph nodes. A major process associated with tumor growth and metastasis is angiogenesis - the formation of new capillaries and generation of blood vessels. This process is essential for the development of the tumor vasculature, which preserves nutrient supply and allows for the drainage of waste (3). Angiogenesis also plays a major role in invasion and metastasis by providing the tumor cells a vascular access to distant targets. A comprehensive research of angiogenesis during tumor progression and metastasis using non-invasive means can help identify the main processes and "actors" in this complex interplay. In this work, *in-vivo* MRI methods were used to monitor breast cancer progression and metastasis in an animal model. We concentrated mainly on metastasis to the bone, which is a preferential site for breast cancer metastasis.

Methods

Human breast cancer cells MDA-MB-231 were orthotopically inoculated (1×10^7) in the mammary glands of SCID mice. All animal procedures were performed according to the regulations of the committee on animals at the Weizmann institute of science. Prior to imaging mice were anesthetized with 1% isoflurane and the legs were stretched in order to image the bones in the same plane. The MR experiments were performed on a 4.7T Biospec spectrometer (Bruker). Images were acquired in a field of view of 5X5 and matrix size of 256 x 128 extrapolated to 256x256. The imaging protocol consisted a T₁-weighted axial 3D gradient-echo sequence (TR/TE = 18.3/4.3ms, flip angle, 30°, acquisition time, 37sec) acquired pre-contrast and a dynamic acquisition for 30 min after a bolus injection of GdDTPA (0.5 mmol/kg weight). Comprehensive evaluation of the contribution of different factors to the contrast enhancement as well as model based analysis (4) yielded parametric images of the transcapillary transfer constant (K^{trans}) and extravascular extracellular volume fraction accessible to the contrast agent (EVF). The MRI results were assessed by comparison with histology findings.

Results

Metastases were detected in H&E stained sections of the lungs, bones and lymph nodes 32-46 days after cell inoculation. The volume and histopathological features of the primary tumors were determined by analyzing their T₂-weighted images. The primary tumors also exhibited a central cyst as was previously described (5). The K^{trans} and EVF parametric images of the primary tumors demonstrated high inter- and intra-tumoral heterogeneity. Metastasis localization was detected in histological slices of the bones, sectioned and screened every 80-100 microns. The metastases loci in the MR images were identified in maximal enhancement maps and were found to correlate with metastasis loci in the histological sections (Figure 1). Analysis of the data using the model-based approach generated K^{trans} and EVF maps in the identified metastatic loci (Figure 2). The K^{trans} and EVF values of bone metastases were similar to those of the primary tumor in its progressed stage, at which metastases were detected (Average values shown in Table 1). Further analyses of the data also indicated disparity in the influx and outflux transfer constants in the primary tumors, suggesting the presence of elevated interstitial pressure. Interstitial hypertension could contribute to the high metastatic potential of these tumors.

Figure 1

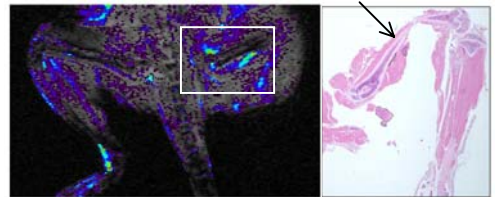
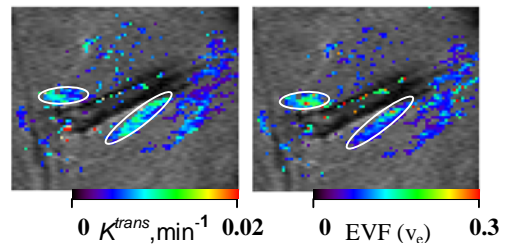


Figure 2



| Table 1: | $K^{trans}, \text{min}^{-1}$ | EVF |
|------------------|------------------------------|-----------------|
| Primary (n=6) | 0.011 ± 0.006 | 0.16 ± 0.04 |
| Metastases (n=7) | 0.009 ± 0.003 | 0.11 ± 0.01 |

Conclusion

We have demonstrated, in an animal model, the capacity of high-resolution contrast enhanced MRI to detect small loci of metastasis of breast cancer to the bone. Furthermore, high similarity between the vascular properties of the primary and the secondary tumors was detected, suggesting similar mechanisms of angiogenic processes in both sites. This similarity in the vascular properties may further help in detection of breast cancer metastases.

References

1. Meyer and Hart Eur J Cancer, 34: 214-221., 1998.
2. Yoneda Eur J Cancer, 34: 240-245., 1998.
3. Carmeliet and Jain Nature, 407: 249-257, 2000.
4. Tofts Brix Buckley Evelhoch Henderson Knopp Larsson Lee Mayr Parker Port Taylor and Weisskoff J Magn Reson Imaging, 10: 223-232., 1999.
5. Dadiani Margalit Sela and Degani, H. Proc Int Soc Magn Med, 11:1234, 2003.